Pulse-analysis-pulse investigation of femtosecond laser-induced periodic surface structures on silicon in air

J. Vincenc Oboňa,[1,*] J. Z. P. Skolski,[1] G. R. B. E. Römer,[2] and A. J. Huis in `t Veld[2]

[1] *Materials innovation institute M2i & University of Twente, Faculty of Engineering Technology, Chair of Applied Laser Technology, P.O. Box 217, 7500 AE, Enschede, The Netherlands*

[2] *University of Twente, Faculty of Engineering Technology, Chair of Applied Laser Technology, P.O. Box 217, 7500 AE, Enschede, The Netherlands*

[*] *j.vincencobona@utwente.nl*

Abstract: A new approach to experimentally investigate laser-induced periodic surface structures (LIPSSs) is introduced. Silicon was iteratively exposed to femtosecond laser pulses at λ = 800 nm and normal incidence in ambient air and at a fluence slightly over the single-pulse modification threshold. After each laser pulse, the topography of the surface was inspected by confocal microscopy. Subsequently, the sample was reproducibly repositioned in the laser setup, to be exposed to the next laser pulse. By this approach, the initiation and spatial evolution ("growth") of the LIPSSs were analyzed as function of the number of pulses applied. It was found that, after the first laser pulses, the ridges of the LIPSSs elevate, and valleys between the ridges deepen, by a few tens of nanometers relative to the initial surface. An electromagnetic model, discussed in earlier works, predicted that the spatial periodicity of LIPSSs decreases with the number of laser pulses applied. This implies material transport and reorganization of the irradiated material on the surface, due to each laser pulse. However, our experiments show a negligible shift of the lateral positions of the LIPSSs on the surface.

OCIS codes: (140.7090) Ultrafast lasers; (180.1790) Confocal microscopy; (240.6680) Surface plasmons.

References and links

1. M. Birnbaum, "Semiconductor surface damage produced by ruby lasers," J. Appl. Phys. **36**(11), 3688–3689 (1965).
2. B. Dusser, Z. Sagan, H. Soder, N. Faure, J. P. Colombier, M. Jourlin, and E. Audouard, "Controlled nanostructrures formation by ultra fast laser pulses for color marking," Opt. Express **18**(3), 2913–2924 (2010).
3. G. Daminelli, J. Krüger, and W. Kautek, "Femtosecond laser interaction with silicon under water confinement," Thin Solid Films **467**(1-2), 334–341 (2004).
4. J. Reif, O. Varlamova, and F. Costache, "Femtosecond laser induced nanostructure formation: self-organization control parameters," Appl. Phys., A Mater. Sci. Process. **92**(4), 1019–1024 (2008).
5. A. Y. Vorobyev and C. Guo, "Colorizing metals with femtosecond laser pulses," Appl. Phys. Lett. **92**(4), 041914 (2008).
6. D. Scorticati, G.-W. Römer, D. F. de Lange, and B. Huis in `t Veld, "Ultra-short-pulsed laser-machined nanogratings of laser-induced periodic surface structures on thin molybdenum layers," J. Nanophotonics **6**(1), 063528 (2012).
7. J. Eichstädt, G. R. B. E. Römer, and A. J. H. in't Veld, "Towards friction control using laser-induced periodic surface structures," Phys. Procedia. **12**, 7–15 (2011).
8. E. Rebollar, I. Frischauf, M. Olbrich, T. Peterbauer, S. Hering, J. Preiner, P. Hinterdorfer, C. Romanin, and J. Heitz, "Proliferation of aligned mammalian cells on laser-nanostructured polystyrene," Biomaterials **29**(12), 1796–1806 (2008).
9. J. E. Sipe, J. F. Young, J. S. Preston, and H. M. van Driel, "Laser-induced periodic surface structure. I. theory," Phys. Rev. B **27**(2), 1141–1154 (1983).

#205750 - $15.00 USD Received 30 Jan 2014; revised 28 Mar 2014; accepted 1 Apr 2014; published 9 Apr 2014

10. J. Z. P. Skolski, G. R. B. E. Römer, J. V. Obona, V. Ocelik, A. J. Huis in 't Veld, and J. T. M. De Hosson, "Laser-induced periodic surface structures: fingerprints of light localization," Phys. Rev. B **85**(7), 075320 (2012).
11. J. Bonse, J. Krüger, S. Höhm, and A. Rosenfeld, "Femtosecond laser-induced periodic surface structures," J. Laser Appl. **24**(4), 042006 (2012).
12. M. Huang, F. Zhao, Y. Cheng, N. Xu, and Z. Xu, "Origin of laser-induced near-subwavelength ripples: interference between surface plasmons and incident laser," ACS Nano **3**(12), 4062–4070 (2009).
13. J. Bonse and J. Krüger, "Pulse number dependence of laser-induced periodic surface structures for femtosecond laser irradiation of silicon," J. Appl. Phys. **108**(3), 034903 (2010).
14. J. Bonse, A. Rosenfeld, and J. Krüger, "On the role of surface plasmon polaritons in the formation of laser-induced periodic surface structures upon irradiation of silicon by femtosecond-laser pulses," J. Appl. Phys. **106**(10), 104910 (2009).
15. J. Z. P. Skolski, G. R. B. E. Römer, J. Vincenc Obona, and A. J. Huis in 't Veld, "Modeling laser-induced periodic surface structures: FDTD-feedback simulations," J. Appl. Phys. **115**, 103102 (2014).
16. A. Borowiec, M. Couillard, G. A. Botton, and H. K. Haugen, "Sub-surface damage in indium phosphide caused by micromachining of grooves with femtosecond and nanosecond laser pulses," Appl. Phys., A Mater. Sci. Process. **79**, 1887–1890 (2004).
17. H. M. van Driel, J. E. Sipe, and J. F. Young, "Laser-induced coherent modulation of solid and liquid surfaces," JOL **30**, 446–471 (1985).
18. L. V. Zhigilei, http://www.faculty.virginia.edu/CompMat/Resources.html.

1. Introduction

Fundamental understanding of the physical phenomena driving the initiation and growth of laser-induced periodic surface structures (LIPSSs) has been the subject of significant scientific interest since the first observation of LIPSSs in 1965 by Birnbaum [1]. The creation of LIPSSs in one non-contact manufacturing step in ambient or other atmospheres and on various materials (air-metal [2], water-semiconductor [3], vacuum-dielectrics [4] etc.) offers great potential in the field of optics, mechanics and biomedical applications. Examples of applications of LIPSSs include, but are not limited to, colorizing and decorating surfaces [2], light trapping [5,6], modification of contact mechanics [7], as well as stimulation and directing the growth of living cells [8].

The first comprehensive theoretical model explaining the properties, i.e. the periodicity and orientation of LIPSSs was developed by Sipe et al. in 1983 [9]. It is based on the interaction of electromagnetic waves with a rough surface. This model, as well as the version extended by Skolski et al. [10] can explain a variety of periodicities and directions of LIPSSs, depending on the irradiation conditions. This paper addresses low spatial frequency LIPSSs (LSFLs) because these are the LIPSSs easily observable in our experiment, therefore the only ones relevant for discussion. LSFLs have a periodicity slightly lower than the wavelength of the incidence light and an orientation orthogonal to polarization of the laser light.

An extensive overview of experiments on the evolution ("growth") of LIPSSs, for a large variety of materials and process conditions, as function of the number of pulses, can be found in a paper from Bonse et al. [11], as well as in a paper from Huang et al. [12]. It was found that the periodicity of LSFLs decreases with an increasing number of pulses applied to the surface. This relation between the periodicity and the number of pulses was explained as a grating-assisted coupling between surface plasmon polaritons (SPPs) and the laser radiation in Ref [12]. It was claimed that a strong increase of this coupling occurs when the number of pulses increases, resulting in a remarkable decrease of the periodicity and increase in the aspect ratio of LSFLs, i.e. a deepening of the LSFLs. However, this decrease in periodicity would necessarily require a transport of surface material, which would be observable from the pulse-to-pulse evolution by lateral shift of the ridges of LSFLs on the surface.

Therefore, in this paper a pulse-analysis-pulse (PAP) experiment is introduced, to experimentally falsify or confirm the above mentioned hypothesis, concerning the lateral shift of LSFLs. This experiment involves alternating steps of surface analysis and the exposure of the surface to successive laser pulses at the same location. This offers a detailed insight into the spatial evolution of the surface topography as function of the number of pulses applied.

#205750 - $15.00 USD Received 30 Jan 2014; revised 28 Mar 2014; accepted 1 Apr 2014; published 9 Apr 2014

2. Experimental setup

A Titanium:sapphire based laser system (Vitesse Duo & RegA 9000 of Coherent) was employed. This source generated 130 fs, linearly polarized, laser pulses with repetition rate of 50 kHz, at a central wavelength of 800 nm. A 1 inch silicon wafer was used as a substrate. The laser beam was delivered to the Si surface at normal incidence by the use of a Galvo-scanner head (SCANgine 14 of SCANLAB) equipped with a 100 mm f-theta lens, which focused the beam to a spot of 9.29 ± 0.06 μm ($1/e^2$) radius. The fluence was controlled by a combination of a polarizing cube and a λ/2 plate (Thorlabs) and was set to 0.56 J/cm^2 in all experiments.

In order to allow easy handling and manipulation, the silicon wafer was glued with colloidal carbon (SPI supplies) on top of an aluminum support plate of 30 × 30 × 10 mm^3. To ensure a reproducible and accurate repositioning of the sample, after each analysis step, the sample with aluminum support was subsequently positioned against 3 alignment pins on the processing table under the laser beam (see Fig. 1(left)).

The repositioning accuracy of the sample was found to be better than ± 1.25 μm. The main contributing factor to this inaccuracy was identified as a friction between the aluminum support plate and the 3-pin-holder (see Fig. 1). The contributions of mechanical vibrations and the spot positioning errors of the Galvo-scanner to these inaccuracies were identified to be negligible. The sample was cleaned prior to the experiments in an ultrasonic bath (Bandelin electronic of Sonorex) at room temperature in four sequential steps of 10 min each: acetone, isopropanol, ethanol and deionized water. After cleaning, the sample was dried using pressurized 1,1,1,2-Tetrafluoroethane. After each irradiation step, the morphology of the Si sample surface was inspected by confocal laser scanning microscopy (CLSM, VK-9700K of Keyence) with 408 nm laser light wavelength providing a height resolution of 1 nm according specification. To accurately align both the CLSM intensity and CSLM height images, alignment marks were used (see Fig. 1(right)). The final alignment of the images was ensured by the use of a graphics editing program. The periodicity of LSFLs was derived from the Fourier transform (FT) of the measured CLSM height data.

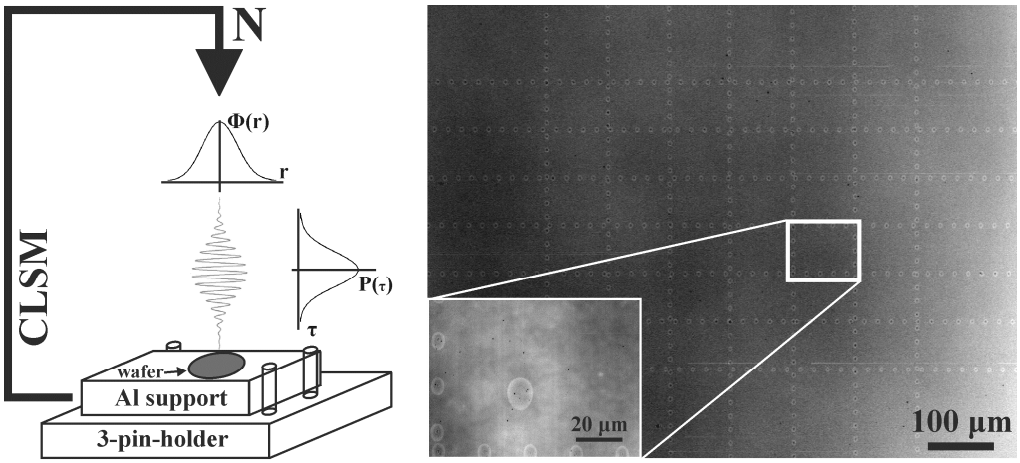

Fig. 1. Sketch of PAP experimental approach: (left) a laser pulse with a spatial, as well as temporal, Gaussian profile irradiates the Si wafer, which is glued to an aluminum support, which in turn, is positioned against 3 alignment pins. (right) After every irradiation step, the surface of the sample was inspected by CLSM. A set of alignment marks were machined on the Si surface prior to the PAP experiments, in a checkerboard pattern. The inset shows a CLSM intensity image at 150 × magnification, after the first pulse. This area of about 90 × 70 μm^2 was used for alignment of all CLSM images in this paper.

#205750 - $15.00 USD Received 30 Jan 2014; revised 28 Mar 2014; accepted 1 Apr 2014; published 9 Apr 2014

3. Results

Figure 2 shows CLSM images of the initial surface conditions and ten subsequent pulses applied to the same location.

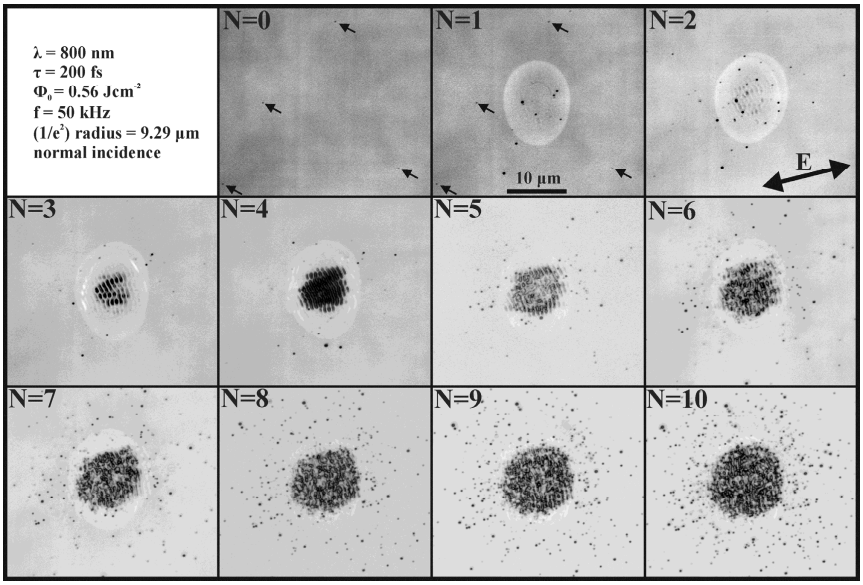

Fig. 2. CLSM intensity images of the silicon surface after a sequence (i.e. number N of) laser pulses applied to the same position on the sample. The number of pulses is indicated in the upper left of each image. The arrows in the image corresponding to N = 0 (no laser pulses, initial surface) and N = 1 intensity images helped to track a change in the number of particles and their positions before and after the first pulse. The double-headed arrow in the N = 2 image indicates the polarization direction of the laser radiation (Media 1).

The first pulse (N = 1) induces two concentric circular areas (or rings) on the surface (see also Fig. 3). Here, the outer, brighter, area was found to be at the same level as the surrounding unprocessed surface. The inner area was found to be approximately 17 nm below the initial surface, as well as bordered with a rim, which is elevated 10 nm over the initial surface.

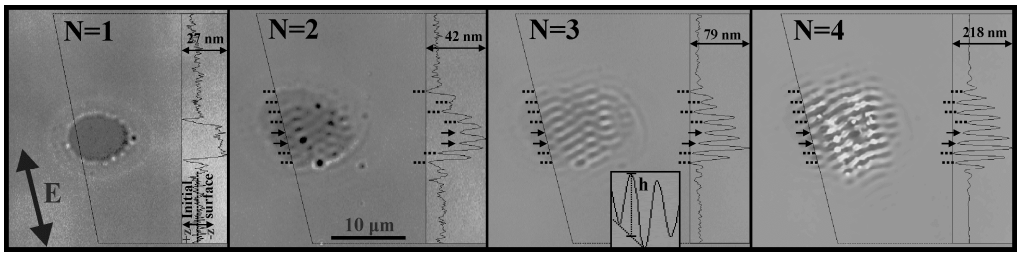

Fig. 3. CLSM height images of the first four pulses, as well as the height profiles to the right of each image, measured at the indicated line across the surface modification. The indicated lines after the 2nd, 3rd and 4th pulse have the same length and exactly the same position. This allows comparison of the height profile of LSFLs, as well as the lateral positions (short dashed lines) of LSFLs. The small double-headed arrows indicate the peak-to-valley distance of the profile. The two single-headed arrows placed on the profile indicate specific ridges of the LSFLs and aid to trace their growth. The inset in the N = 3 image depicts the way the height of these two LSFLs was measured. The evolution of the height (h in N = 3 image) is as follows (lower arrow, upper arrow): 17 nm and 16 nm for N = 2, 67 and 49 nm for N = 3, 191 nm and 180 nm for N = 4.

By comparison of N = 1 and N = 2 in Fig. 3 can be concluded that the second pulse does not have a significant effect on height of the rim around the inner area. However, the central

#205750 - $15.00 USD Received 30 Jan 2014; revised 28 Mar 2014; accepted 1 Apr 2014; published 9 Apr 2014

part of the crater is further deepened by the second pulse and reaches 33 nm under the original surface level. Moreover, this second pulse initiates the first LSFLs. The height of these LSFLs is sub-20 nm and the ridges do not exceed the initial surface. The 3rd pulse elevates the rim slightly to 13 nm. The ridges of the LSFLs in the center of the spot are at almost the same height as the surrounding surface and the deepest valley is at 66 nm below the initial surface. Further, LSFLs are observed at larger distances from the center of the spot, in comparison to the case after two laser pulses (N = 2). The 4th laser pulse elevates the ridges of the LSFLs to 62 nm above the initial surface and deepens the valleys to 156 nm below the surface. A nonlinear increase of the height profiles can be observed with increasing number of laser pulses (Fig. 3). As of the 4th laser pulse, a disordering of the LSFLs in the center of the spot is observed. This disorder is accompanied with a creation of spherical drops on the ridges of the LSFLs. The LSFLs in the center of the spot are progressively disintegrating from the 5th pulse onward, but they are still visible at the margins of the spot (Media 1).

The confocal intensity images in Fig. 2 can also be used to study the number of the surface re-deposited particles and their (re)location on a pulse to pulse basis. When in Fig. 2 image N = 0 is compared to image N = 1, it can be concluded that re-deposited spherical particles were produced even by the 1st pulse. As the depth of crater after the 1st pulse is 17 nm, re-deposition is to be expected. The number of particles increases slightly from the 1st to the 4th and 5th pulse. A significant number of particles are observed after the 5th pulse. This increase can probably be attributed to the disintegration of LSFLs, rather than to the deepening of the surface structures.

Next, the volume of material, which moves on, or is removed from, the modified surface was determined. Figure 4 (right), shows the volume of material below the surface level (V_{BSL}), the volume of material above the surface level (V_{ASL}) and the difference of these volumes ΔV, as function of the number of pulses. The difference volume ΔV is the volume of material which is removed from the laser-material interaction zone in form of particles or vapor. The increase of V_{BSL} after the 2nd pulse can be attributed to the enhanced absorption of laser light by the corrugated surface due to the presence of LSFLs. From the 4th pulse onwards, V_{BSL} increases nearly linearly as the ablation crater deepens. The volume of material above the surface V_{ASL} is nearly constant up to and including the 3rd pulse, which can be attributed to the volume of the elevated rim that gives the main contribution to this volume. A significant increase of V_{ASL} as of the 4th pulse implies that the LSFLs ridges protrude above the original surface, whereas these ridges were below the surface up to the 4th pulse. This is consistent with observations in Fig. 3.

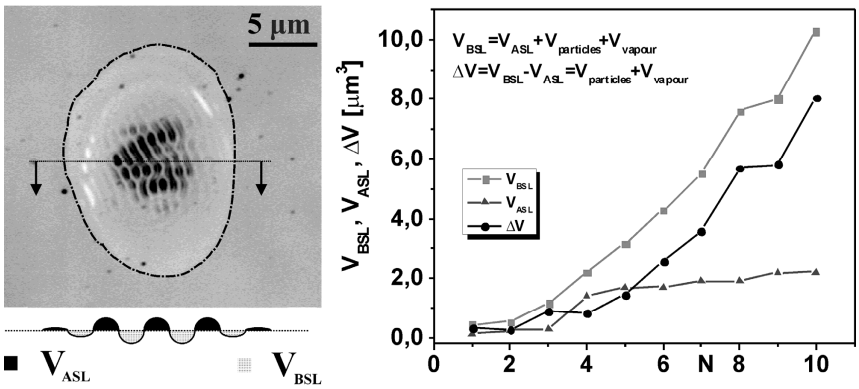

Fig. 4. Measured volumes, based on CLSM height images. (left) The volumes were measured in modified area (dashed-dot line). Below this image, in the schematic representation of the cross-section of LSFLs, the volume below the surface level (V_{BSL}) and the volume above the surface level (V_{ASL}) are defined. (right) The volume V_{BSL}, V_{ASL} as well as, their difference ΔV, as function of the number of pulses applied. ΔV represents the volume of material removed from the laser-material interaction zone due to laser irradiation.

#205750 - $15.00 USD Received 30 Jan 2014; revised 28 Mar 2014; accepted 1 Apr 2014; published 9 Apr 2014

From the 4th pulse, the V_{ASL} increases only slightly for increasing number of pulses. This can be attributed to the disintegration of LSFLs in the center of the spot. Only random material jets in the center of the spot, and the elevated rim contribute to this volume. The increase of the difference volume ΔV due to the first 4 to 5 pulses is small compared to ΔV from the 5th pulse and up. This trend is in agreement with the qualitative observation of the number of particles on the surface (Fig. 2). An interesting detail can be observed between the 3rd and the 5th pulse where V_{ASL} exceeds ΔV. It implies that more material is "pushed" into the ridges of the LSFLs than is removed from the laser-material interaction zone.

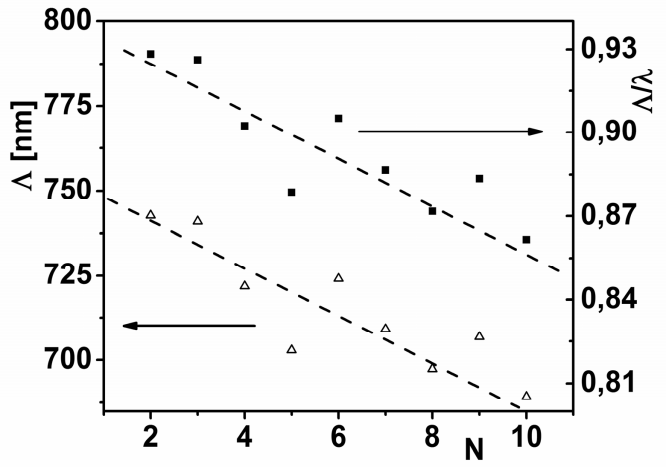

Fig. 5. Spatial periodicity Λ of the LSFLs (open triangles), as well as the normalized periodicity Λ/λ (solid squares), as function of the number of pulses. λ = 800nm is the wavelength of the laser radiation. The dashed lines (not a linear fit) provide a guide to the eye in order to discern a decrease of periodicity with increasing number of pulses N.

Figure 5 shows the effect of the number of laser pulses N on the spatial periodicity Λ, as well as the normalized periodicity Λ/λ, of the LSFLs. The Λ was determined from FT of the full area of the CLSM height images. However, this graph should be taken as a semi-quantitative representation of the experimental results, because it is based on only a small number of LSFLs in the CLSM height maps. The normalized periodicity Λ/λ value decreases from 0.93 to 0.86 between the 2nd and the 10th pulse. This is associated with the disintegration of the LSFLs in the center of the spot. In other words, this trend implies that the periodicity of the LSFLs located at the spot margin, dominates in the FT of the LSFLs at high number of pulses. The disintegrated surface features from the center of the laser spot, have a negligible contribution to the amplitude of the relevant Fourier coefficients.

4. Discussion

The dependence of the spatial periodicity of LSFLs on the laser parameters has been studied for many materials in literature [11,12]. The general trend is that the periodicity of LSFLs decreases with an increasing number of pulses. This phenomenon has been attributed to the combination of three effects in literature: (1) a decrease of the excitation of the material from the center to the margin of the spot, caused by a Gaussian profile of the beam [12,13]; (2) a possible change of the angle of incidence of the laser light at the edges of the ablated crater [13]; and (3) grating-assisted SPP-laser coupling [12,13].

The first effect seems to be well understood from Bonse et al. [14], as well as Skolski et al. [15], where the dependence of the periodicity of LSFLs on the surface excitation has been shown by modelling. The reader should keep in mind that LSFLs created in the center of a laser spot, at high fluence, have a higher periodicity than the LSFLs created in the margin of a laser spot, at lower fluence [12–15]. However, LSFLs are continuously disintegrated in the center of the spot, with increasing number of pulses. It means that the FTs of the SEM

#205750 - $15.00 USD Received 30 Jan 2014; revised 28 Mar 2014; accepted 1 Apr 2014; published 9 Apr 2014

micrographs of surfaces exposed to higher number of pulses, contain information about the periodicities of LSFLs closer to the margin of the spot mainly, i.e. smaller periodicities (see Fig. 2(c) in [13]). The second effect, concerning the change of angle of incidence, may be excluded in the present experiment, since the ablation crater starts to deepen only after the 5th pulse (start of the disintegration of LSFLs) and the decrease of the periodicity of LSFLs is visible already for N from 2 to 5. Moreover, even for N from 6 to10, the crater is very shallow. Then, the third effect of grating-assisted SPP-laser coupling is only one remaining for this discussion.

Huang et al. [12] showed in simulation results on wide band-gap semiconductor ZnO that, the coupling of laser light in 60 nm deep valleys does reduce the periodicity of the modulated absorption profile by a significant 40% factor. This can be expected only if a major reorganization of surface material occurs in the laser-material interaction zone on a pulse-to-pulse basis. That is, for instance, by complete melting of the surface structures and their subsequent (re-)growth from the molten layer. This implies that a lateral shift of these structures should be observable on the surface. In this paper a PAP experiment is introduced, to experimentally falsify or confirm the above mentioned hypothesis regarding the lateral shift of LSFLs. It provides the following four main results:

- The non-linear coupling of the laser energy with the surface creates LSFLs with heights (see increase of h in Fig. 3) larger than 200 nm, after the first few pulses.
- The most significant growth of LSFLs is accompanied by large volumes of material "pushed" into the ridges of LSFLs. These volumes are larger than the volumes of material removed from the laser-material interaction zone.
- The ridges of the LSFLs show negligible shifts in lateral positions.
- The periodicity of the LSFLs slightly decreases with an increasing number of laser pulses, where the lower values of the periodicity correspond to LSFLs in the margin of the laser-material interaction zone.

It can be concluded that the "growth" of LSFLs progresses as material is "pushed" from valleys to ridges. The conditions for a significant reduction of the periodicity of the LSFLs should be met, according to [12], already after the third pulse. However, a lateral shift of the LSFLs has not been observed in the PAP experiments. It shows that the effect (1), variation in the surface excitation, seems to be sufficient for explanation of the periodicity differences.

Finally, three additional references are relevant in order to support our experimental observations, as well as to better understand the evolution of LSFLs. That is, Borowiec et al. [16] showed that LSFLs, when processed with iterative femtosecond irradiation, were covered with only a thin layer of re-solidified material and the major part of this material was present on the tops of the LSFLs. Another argument supporting our findings can be derived from the results of van Driel et al. [17]. These authors suggest that melting and re-solidification of a continuous layer of material creates "sombrero-like" structures on the surface as a result of inhomogeneous deposition of energy in the solid and an action of surface tension in the melt. Once these "sombrero-like" corrugations appear, the energy of the subsequent laser pulse tends to be absorbed in the valleys, not at the "sombreros" top. It would result in creation of the sombreros at different locations. Movement of LSFLs was not present in our experiment thus we exclude full melting of these structures. The last argument originates from a model of the laser-matter interaction provided by the group of Zhigilei [18]. Their research has been focused on processes induced with laser pulses on the surface of various materials. They combined the two-temperature model with molecular dynamics (TTM-MD) and identified three regimes of material transport/removal depending on the level of absorbed fluence only - i.e. melting, spallation and phase explosion. "Growth" of LSFLs may be then understood as follows: (*i*) after initiation of LSFLs on the surface, the energy of the subsequent laser pulses start to be absorbed at fixed locations in the valleys of LSFLs; (*ii*) a mix of melting, spallation and phase explosion induces expansion of the irradiated material which "pushes" the material towards tops of the LSFLs; (*iii*) enhanced absorption of the

#205750 - $15.00 USD Received 30 Jan 2014; revised 28 Mar 2014; accepted 1 Apr 2014; published 9 Apr 2014

energy in the progressively deeper valleys may potentially either reduce lateral dimension (width) of the solid ridges or even melt the ridges through, destroying the ridges due to extensive forces of the expanding material in the valleys.

4. Conclusion

The experimental work presented in this paper was focused on achieving an increased understanding of the initiation and growth of laser-induced periodic surface structures (LIPSSs). A silicon wafer was irradiated with ultra-short laser pulses: 130 fs laser pulses, 50 kHz repetition rate, 800 nm wavelength, peak fluence of 0.56 J/cm^2, 9.29 ± 0.06 μm 1/e^2 beam radius, linear polarization and normal incidence. The sample was repeatedly placed to the same position on laser table and irradiated to the same spot with laser pulses. It enabled investigation of the evolution of the surface topography on a pulse-to-pulse basis. Precise alignment of intensity and height confocal microscopy images before the 1st and after each additional laser pulse made comparison of the LIPSSs lateral positions straightforward. The main results of this investigation may be summarized as follows:

- The ridges of low spatial frequency LIPSSs (LSFLs) can grow above the initial surface.
- The growth of LSFLs, during the first few pulses (N from 3 to 5 in this experiment), is accompanied with a "push" of material from the valleys between the LSFLs to the ridges of the LSFLs. This process dominates over the ablation.
- The LSFLs are visible only in an annular region of the laser spot for higher number of laser pulses.
- The lateral positions of the ridges of LSFLs showed negligible changes during their growth.

The observation of negligible lateral shifts of the ridges of LSFLs with an increasing number of pulses is the main outcome. Results show that grating-assisted SPP-laser coupling is not necessarily needed to explain the drop of periodicity of LSFLs, when subsequent laser pulses are applied.

Acknowledgment

This research was carried out in the framework of the Research Program of the Materials innovation institute M2i (www.m2i.nl) under project number M61.3.08300.

#205750 - $15.00 USD Received 30 Jan 2014; revised 28 Mar 2014; accepted 1 Apr 2014; published 9 Apr 2014